Received: December 27, 2019
Revised: February 10, 2020
Accepted: February 17, 2020

Sputtering of Crystalline ZrN Thin Films on Unheated Substrates for Decorative coating Applications

Mano Valaiauksornlikit[1], Worawarong Rakreungdet[2], Chanunthorn Chananonnawathorn[3], Saksorn Limwichean[3], Pitak Eiamchai[3], Tossaporn Lertvanithphol[3], Noppadon Nuntawong[3], Viyapol Patthanasettakul[3], Mati Horprathum[3,*]

[1]*Department of Physics, Faculty of Science, King Mongkut's University of Technology Thonburi, Bangkok, 10140, Thailand*

[2] *The Institute for the Promotion of Teaching Science and Technology (IPST), KlongToey, Bangkok, 10110, Thailand*

[3]*National Electronics and Computer Technology Center (NECTEC), National Science and Technology Development Agency (NSTDA), Pathumthani 12120, Thailand*

Abstract

The zirconium nitride (ZrN) thin films were successfully deposited by the DC reactive magnetron sputtering without heat treatment for the hard-coating applications. The ZrN thin films were carefully prepared at 200 nm under different operating pressures. The obtained films were systematically analyzed for physical, electrical, and optical properties, and discussed to the operating pressures. For the crystal structures, the XRD results indicated that most ZrN films were cubic close-packed structure with (111) and (220) orientations. Only the film prepared at the smallest operating pressure showed three phases of (111), (200), and (220) according to the localized heating from high atomic energy. For the film morphologies, the FE-SEM results demonstrated the increase of densely packed structure and the decrease of the surface roughness for the films prepared at low operating pressures. The film resistivity was found closely related to the electron scattering in the grain boundaries, as well as with the thin-film brightness. The optical properties of the films were determined from the reflection, lightness, and yellowness, as observed in the CIE chromaticity diagrams.

Keywords: Zirconium nitride thin film, Sputtering, Lightness, Decorative

1. Introduction

With the constant developments of the industrial and consumer machinery, surface treatment technology is a significant method to improve the durability of components, tools, molds, and machine parts, which have been used in mechanical, electronic, optical and decorative applications. One of the major interests in the surface treatment is metal nitrides because they appear in a gold-like color and are generally used in both the hard and decorative coatings. The metal nitrides are usually prepared with the fourth-column (IV) transition metals, i.e., titanium (Ti), hafnium (Hf), and zirconium (Zr), because of excellence in hardness, young's modulus, and tribological interactions [1-2]. Among these metal nitrides, zirconium nitride (ZrN) is one of the most attractive because of its excellent chemical and physical properties [3]. Also, ZrN demonstrates unique characteristics, i.e., high hardness up to 23.5 GPa [4], high optical reflection up to 80% in the infrared region [5], the visual color of light-yellowness [6], low resistivity of $\rho \approx 13.6$ μΩ·cm at 300 K [7], and applicable as Josephson junctions and diffusion barriers [8]. In addition, ZrN has a high melting point at 2,980 °C, and high thermal stability of ΔH = -87.3 kcal mole^{-1} [9].

To utilize ZrN material in both hard-coating and decorative applications, ZrN thin films are widely studied. Numerous techniques that have been reported include chemical vapor deposition (CVD) [10], pulse laser deposition [11], ion-beam assisted deposition [12], and hollow cathode discharge ion planting (HCP-IP) [13]. One of the most widely studied deposition process to prepare the ZrN films is physical vapor deposition (PVD), especially a pulsed dc magnetron sputtering, which can be easily adapted to large-area coatings. The sputtering technique, generally performed with a Zr target in argon and nitrogen gases, can effectively control the thin film properties from the deposition conditions. Unfortunately, without an external substrate heating and negative substrate bias, as-deposited ZrN thin films are mostly amorphous because the Zr-N system contains phases such as Zr_3N_4 that can be amorphous [5, 14-16]. To promote film crystallinity, the ZrN films need high-temperature post-annealing treatment, substrate heating, or negative substrate bias during the film deposition [17-20]. Until recently, few groups have successfully fabricated high-quality ZrN thin films without the substrate heating or the negative substrate bias for the desired material properties [21-23]. Their technique has been known as a low-temperature crystalline deposition, which is of particular interest in most thin-film industries. With such a technique, they can reduce production costs when minimum requirements for substrates with high-temperature tolerance are needed.

In this work, we, therefore, examined the growth of crystalline ZrN thin films on the unheated substrates towards the decorative applications. The influence of the operating pressure on several characteristics, i.e., the structural, the morphological, the optical, and the electrical resistivity of the reactively sputtered ZrN films were thoroughly investigated and discussed.

2. Experimental details

The crystalline ZrN thin films were prepared, without any heat treatment, by the pulsed DC reactive magnetron sputtering (AJA International, Inc.; ATC 2000-F) at the ambient temperature. At 80-mm distance (D_{s-t}) from the substrate holder, the sputtering cathode was tilted at an inclined angle of 40° to the substrate normal to obtain the most optimal film uniformity without biaxial alignment [24]. In this study, identical ZrN films were fabricated on two types of substrates for different purposes, i.e., silicon (100) with a native oxide and glass slide substrates were used for thin-film characterizations. All the substrates were sequentially cleaned in the ultrasonic washer with acetone, isopropanol, and deionized water, and then dried in a nitrogen atmosphere. After being loaded into the deposition chamber, the substrates were cleaned by argon ion plasma for 15 minutes, with an RF power of 30 W at an operating pressure of 0.67 Pa, in order to remove surface contamination. In addition, the Zr target was also pre-sputtered in the argon plasma to remove an excessive oxide surface layer. When the base pressure of the chamber reached 1.33×10^{-5} Pa, high purity argon (99.999 %) and nitrogen (99.999 %) were supplied as sputtering and reactive gases, respectively. Controlled with mass-flow meters (MKS), the flow rates of argon and nitrogen were kept constant at 20 and 2.0 sccm, respectively. For this sputtering system, such choice of gas flow rates was best optimized for the deposition rate and the quality of the ZrN films, while avoiding poisoning effects. During the film deposition, a two-inch diameter Zr (99.995 %) target (K.J. Lesker) was sputtered with the pulsed DC frequency at 20 kHz. The sputtering discharge was then generated at a constant DC pulse power of 400 W. The operating pressures, automatically controlled with a pressure control gate valve, were monitored with Pirani, Baraton, and Penning gauges. Table 1 gives a summary of the film deposition conditions.

Table 1. Deposition parameters for preparation ZrN thin films by dc reactive magnetron sputtering.

Deposition Parameter	
Target material	Zr (99.995 %)
Substrate	Silicon (100), glass slide
Ar flow rate	20 sccm
N_2 flow rate	2 sccm
Based pressure	1.33×10^{-5} Pa
Operating pressure	0.13-2.0 Pa
DC power	400 W
Film thickness	200 nm
Deposition rate	23.5-28.0 nm/min
Deposition time	~7-9 min

The obtained ZrN thin films on the silicon and glass substrates were examined for physical, morphological, electrical, and optical properties. First, crystalline structures of the ZrN films were determined by grazing incidence X-ray diffraction (GIXRD; RIGAKU TTRAX III) operated with a Cu-K_{α}1 source at a grazing incidence of 0.4° and measured at 2° of 30-60°. Next, the cross-sectional and surface morphologies of the films were investigated with field-emission scanning electron microscopy (FE-SEM; Hitachi S-4700). Then, an electrical resistivity was measured by a four-point probe method (Jandel RM3). Color measurements were then performed with HunterLab ColorQuest with an integrating sphere. Colorimetry was carried out under the CIE-L*a*b* method, where L*, a*, and b* represented brilliance, red–green, and blue - yellow coloration, respectively.

3. Results and discussion

In general, the thin films for the hard-coating applications depend mostly on the crystallinity of the materials. In this study, the ZrN thin films were reactively sputtered at different operating pressures, whose effects on the crystal orientations of ZrN have been investigated. Fig. 1 shows the GIXRD patterns of the ZrN thin films deposited on the silicon wafers substrate at the operating pressure ranging from 0.13 to 2.0 Pa. Although from the figure, the XRD intensities depended heavily on the operating pressure during the film deposition, all of the ZrN thin films exhibited a cubic close-packed structure (NaCl-type, ICDD PDF #35-0753) with the (111) and (220) orientations. When the operating pressure was decreased from 2.0 to 0.40 Pa, the XRD peaks of the (111) and (220) planes were constantly increased as a result of higher crystallization in the ZrN films. Such ZrN crystallization can be explained from induced energy sources during the deposition. Although the ZrN films prepared without an external bias and a substrate heating are typical of amorphous or Zr_3N_4 cubic phase [5, 9, 15], two possible approaches to crystallize the ZrN films are (i) the increased energy of particles impinging on the film surface and (ii) the thermal energy induced by the localized substrate heating [25-27]. When the operating pressure was further decreased to 0.13 Pa, however, the ZrN film instead exhibited a decrease of (111), and a slight increase of (220) crystal orientations. In addition, a (200) crystal orientations not present in the other samples were now observed. The characteristic (200) peak represented the stable plane, which occurred thermodynamically from the minimal surface energy. A small fraction of the (200) orientation indicated that ZrN grains could have been formed during the secondary nucleation because of growth-induced defects. Another possible mechanism was a change in growth

kinetics, which caused a more effective collision dissociation of N_2 molecules or N^{2+} ions, providing a higher N coverage in favor of the (200) texture [28, 29].

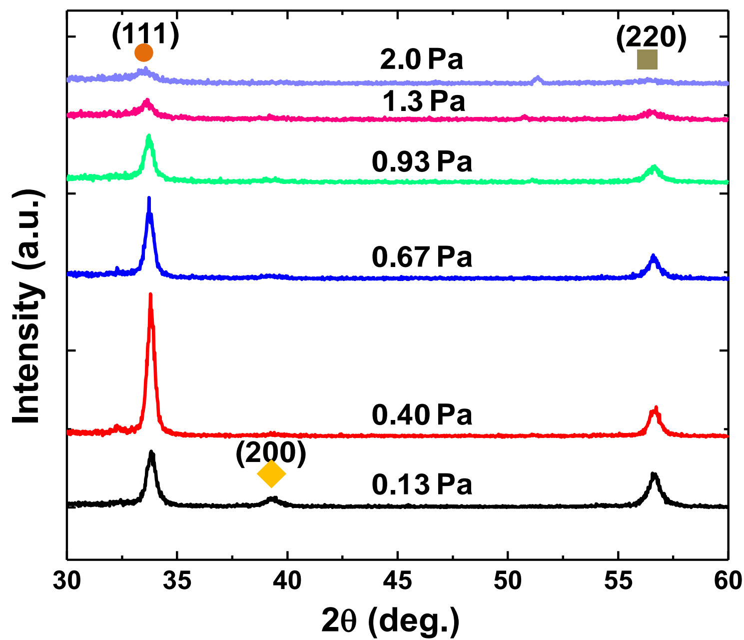

Fig. 1. The XRD patterns of the ZrN thin films, prepared at different operating pressures.

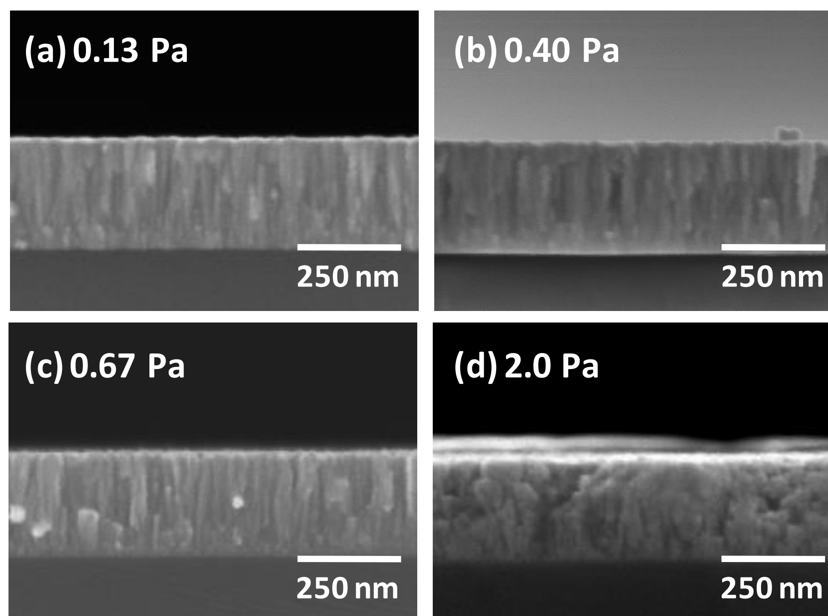

Fig. 2. The surface-topological and cross-sectional FE-SEM images of the ZrN thin films prepared at different operating pressures: (a) 0.13, (b) 0.40, (c) 0.67, and (d) 2.0 Pa.

The effect of the operating pressure during the deposition to the film morphologies of the ZrN thin films on a silicon wafer substrate was investigated with FE-SEM (Fig. 2). The cross-sectional FE-SEM images revealed the ZrN films with a columnar structure, which was consistent with zone T in the structure-zone model [30-31]. The images also confirmed nearly identical film thickness without a significant change in the columnar structures. Further examinations however indicated the change in density of the thin films, especially at the highest operating pressure when open boundaries between columns were observed. The increase in the open boundaries could be well explained from the small energy of the sputtered particles arriving at the substrates, because of the increased number of the scattering particles at that pressure. The lower the energy of the sputtered atoms arriving at the substrates, the smaller the mobility in the growing films, which would demonstrate higher film porosity.

The physical surface of the ZrN thin film on silicon wafer substrates was examined by the AFM in the tapping mode. The root means square (RMS) roughness was calculated and plotted, as shown in Fig. 3. The minimum RMS roughness was observed at the lowest operating pressure which greatly affected the particles' kinetic energy. The maximum roughness was observed at the moderate operating pressure of 0.93-1.33 Pa. At such pressures, the decreased energy of the adatoms consequently lowered their capability to move on the surface of the substrates, which resulted in roughened surface morphologies. Nevertheless, the RMS roughness only varied between 2.4 to 5.0 nm, which was nearly insignificant as also observed from the corresponding AFM images.

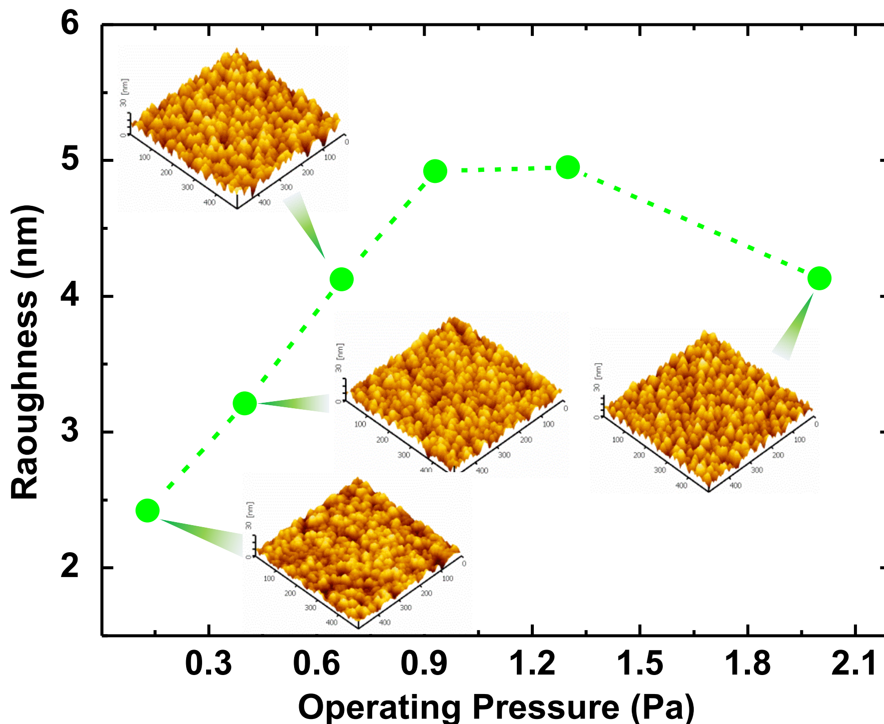

Fig. 3. The RMS roughness of the ZrN thin films measured as a function of the operating pressure. The insets represented the AFM images of the corresponding ZrN thin films.

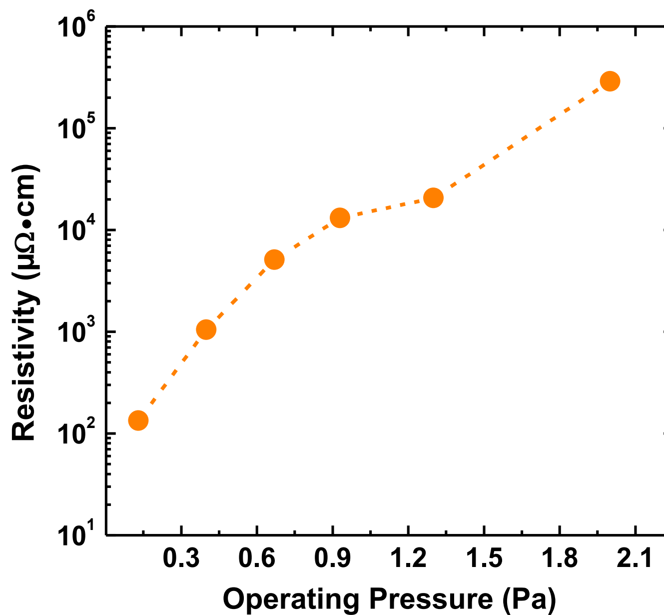

Fig. 4. The resistivity of the ZrN thin films as function of the operating pressure during the film deposition.

The effect of the operating pressure during the ZrN film deposition to the electrical resistivity was shown in Fig. 4. At the highest operating pressure, the ZrN film on glass slide substrate, with the smallest grain size, yielded the largest resistivity at 2.8×10^5 μΩ·cm. When the operating pressure was decreased from 2.0 to 0.40 Pa, the resistivity was logarithmically decreased with the increased grain size. The relation was the result of the decrease of electron scattering in the grain boundaries [17, 19, 32, 33]. The smallest operating pressure of 0.13 Pa, the resistivity was further decreased when the grain size was instead decreased. Such a result was the effect of the ion kinetic energy which was continuously increased due to the increased crystallinity of the ZrN thin films, similar to other publications [15, 17].

Fig. 5 shows the photograph of the ZrN film deposited on a glass slide substrate at different operating pressure. The film color became the light gold to the brown color with increasing operating pressure. The chromaticity of the fabricated ZrN thin films was measured by the colorimeter and converted to the CIE L*a*b*. Because this work also aimed at the decorative coatings, the values of L* and b* were of much interest. In Fig. 6(a), the plots of CIE L*a*b* indicated that, towards the lowest pressure, both the L* and b* were largely increased to 70 and 25, respectively, while a* was slightly decreased toward 0. The results corresponded to direct inspections of the samples whose brightness and yellowness yielded light-gold color. This was the nature of the nitrides associated with the increase of the crystallographic ZrN structure. In Fig. 6(b), the CIE L*a*b* was converted to CIE xyz and plotted as the tritimulus diagram. From the figure, when the operating pressure was continuously decreased, we clearly observed nearly linear transition from light violet color towards brown, and eventually to light-gold color. Such a change in the chromaticity could be explained from the Drude's model for the electronic transition within the films, where the reflectivity of materials and the complex refractive index were related to the number of free d electrons [6, 15, 34].

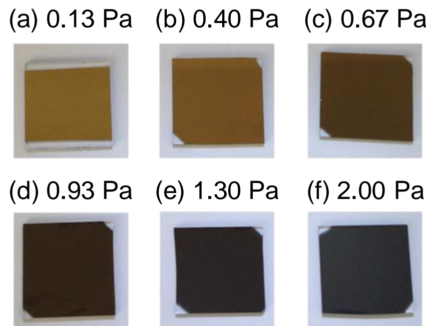

Fig. 5. Photograph of the ZrN thin films deposited on a glass substrate at different operating pressure

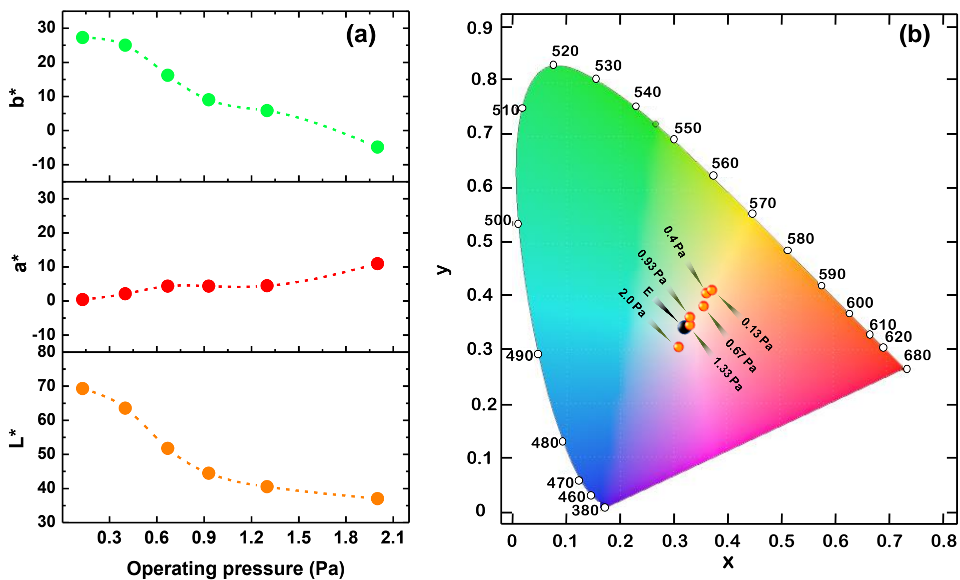

Fig. 6. The chromaticity of the ZrN thin films: (a) CIE L*a*b*, and (b) CIE xyz

4. Conclusion

The ZrN thin films were successfully deposited by the DC reactive magnetron sputtering system at the ambient temperature without further heat treatment. The ZrN films of 200 nm thickness were prepared at different operating pressures and analyzed based on thin-film properties and hardness measurements. From the GIXRD results, all samples were cubic close-packed structure with (111) and (220) orientations. Only the ZrN film prepared at the lowest operating pressure showed the additional (200) plane. With the FE-SEM, the films prepared at low operating pressures demonstrated the increase in the densely packed columnar structure, the surface roughness, and the grain sizes. The film resistivity was closely related to the electron scattering in the grain boundaries of the obtained films. Such electrical properties were eventually related to the optical properties, as observed from the reflection, lightness, and yellowness in the CIE chromaticity diagrams.

Acknowledgment

This work was supported by Functional Material Cross Cutting Technology Program, National Science and Technology Development Agency (NSTDA), Thailand. Mr. Mano Valaiauksornlikit would like to acknowledge financial support from a Thailand Center of Excellence in Physics scholarship.

References

[1] Budke E, Krempel-Hesse J, Maidhof H, Schüssler H. Decorative hard coatings with improved corrosion resistance. Surf. Coat. Technol.1999;112:108-13.

[2] Nowak R, Maruno S. Surface deformation and electrical properties of HfN thin films deposited by reactive sputtering. Mater. Sci. Eng., A. 1995;202:226-37.

[3] Larijani M M, Norouzian Sh, Afzalzadeh R, Balashabadi P, Dibaji H, Effects of post annealing on micro and nanostructural properties of ZrN films prepared by ion beam sputtering technique on SS304. Surf. Coat. Technol. 2009;203:2486-9.

[4] Brugnoni C, Lanza F, Macchi G , Müller R, Parnisari E, Stroosnijder M F, Vinhas J, Evaluation of wear resistance of ZrN coatings using thin layer activation. Surf. Coat. Technol. 1998;100-101:23-6.

[5] Schleussner S, Kubart T, Törndahl T, Edoff M. Reactively sputtered ZrN for application as reflecting back contact in Cu(In,Ga)Se_2 solar cells. Thin Solid Films. 2009;517: 5548-52.

[6] Niyomsoan S, Grant W, Olson D L, Mishra B. Variation of color in titanium and zirconium nitride decorative thin films. Thin Solid Films. 2002;415:187-94.

[7] Wang C C, Akbar S A, Chen W, Patton V D. Electrical properties of high-temperature oxides, borides, carbides and nitrides. J. Mater. Sci. 1995;30:1627-41.

[8] Schwarz K, Williams AR, Cuomo JJ, JH Harper, AH Hentzell, Zirconium Nitride-A New Material for Josephson Junctions. Phys. Rev. B: Condens. 1985;32:8312-16.

[9] Jimènez H, Restrepo E, Devia A. Effect of the substrate temperature in ZrN coatings grown by the pulsed arc technique studied by XRD. Surf. Coat. Technol. 2006;201: 1594-601

[10] Wendel H, Suhr H. Thin zirconium nitride films prepared by plasma-enhanced CVD. Appl. Phys. A. 1992;54:389-92.

[11] Spillmann H, Willmott P R, Morstein M, Uggowitzer P J. ZrN, ZrxAlyN and ZrxGayN thin films - novel materials for hard coatings grown using pulsed laser deposition. Appl. Phys. A. 2001;73:441-50.

[12] Ensinger W, Volz K, Kiuchi M. Ion beam – assisted deposition of nitrides of the 4th group of transition metals. Surf. Coat. Technol. 2000;128-129:81-4.

[13] Huang J-H, Hsu C-Y, Chen S-S, Yu G-P. Effect of substrate bias on the structure and properties of ion-plated ZrN on Si and stainless steel substrates, Mater. Chem. Phys. 2003;77:14-21.

[14] Leu L C, Sadik P, Norton D P, McElwee-White L, Anderson T J. Comparative study of ZrN and Zr–Ge–N thin films as diffusion barriers for Cu metallization on Si. J. Vac. Sci. Technol., B. 2008;26:1723-7.

[15] Benia H M, Guemmaz M, Schmerber G, Mosser A, Parlebas J-C. Investigations on non-stoichiometic, zirconium nitrides. Appl. Surf. Sci. 2002;200:231-8.

[16] Rizzo A, Signore M A, Mirenghi L, Dimaio D. Deposition and properties of ZrNx films produced by radio frequency reactive magnetron sputtering. Thin Solid Films. 2006;515: 1486-93

[17] Liu C-P, Yang H-G. Systematic study of the evolution of texture and electrical properties of ZrNx thin films by reactive DC magnetron sputtering. Thin Solid Films. 2003;444:111-9.
[18] Liu C-P, Yang H-G. Deposition temperature and thickness effects on the characteristics of dc-sputtered ZrN_x films. Mater. Chem. Phys. 2004;86:370-4.
[19] Chen C-S, Liu C-P, Yang H-G, and Tsao Chi Y A. Influence of the preferred orientation and thickness of zirconium nitride films on the diffusion property in copper. J. Vac. Sci. Technol., B. 2004;22:1075-83.
[20] Wang S-H, Chang C-C, Chen J S. Effects of substrate bias and nitrogen flow ratio on the resistivity, density, stoichiometry, and crystal structure of reactively sputtered ZrNx thin films. J. Vac. Sci. Technol., A. 2004;22(5):2145-51.
[21] Pelleg J, Bibi A, Sinder M. Contact characterizations of ZrN thin films obtained by reactive sputtering. Physica B. 2007;393:292-7.
[22] Roman D, Bernardi J, LG de Amorim C, S de Souzac F, Spinelli A, Giacomelli C, Figueroa C A, JR Baumvol I, LO Basso R. Effect of deposition temperature on microstructure and corrosion resistance of ZrN thin films deposited by DC reactive magnetron sputtering. Mater. Chem. Phys. 2011;130:147-53.
[23] Bhuvaneswari, H B, Nithiya Priya, I, Chandramani, R, Rajagopal Reddy, V, Mohan Rao, G. Studies on zirconium nitride films deposited by reactive magnetron sputtering. Cryst. Res. Technol. 2003;38:1047-51.
[24] Horprathum M, Eiamchai P, Chindaudom P, Nuntawong N, Patthanasettakul V, Limnonthakul P, Limsuwan P. Characterization of inhomogeneity in TiO_2 thin films prepared by pulsed dc reactive magnetron sputtering. Thin Solid Films. 2011;520:272-9.
[25] Taga Y, Takahasi R. Role of kinetic energy of sputtered particles in thinfilm formation. Thin Solid Films. 1990;193-194:164-70.
[26] Lee Y E, Lee J B, Kim Y J, Yang H K, Park J C, Kim H J. Microstructural evolution and preferred orientation change of radio-frequency-magnetron sputtered ZnO thin films. J J. Vac. Sci. Technol., A. 1996;14:1943-8
[27] Pradhan S S, Pradhan S K, Bhavanasi V, Sahoo S, Sarangi S N, Anwar S, Barhai P K. Low temperature stabilized rutile phase TiO_2 films grown by sputtering. Thin Solid Films. 2012;520:1809-13
[28] Koutsokeras L E, Abadias G. Intrinsic stress in ZrN thin films: Evaluation of grain boundary contribution from in situ wafer curvature and ex situ x-ray diffraction techniques. J. Appl. Phys. 2012;111:093509.
[29] Gall D, Kodambaka S, Wall M A, Petrov I, and Greene J E. Pathways of atomistic processes on TiN(001) and (111) surfaces during film growth: an ab initio study. J. Appl. Phys. 2003;93:9086-94.
[30] Thornton J A. Influence of apparatus geometry and deposition conditions on the structure and topography of thick sputtered coatings. J. Vac. Sci. Technol., A. 1974;11:666-70.
[31] Thornton J A. Influence of substrate temperature and deposition rate on structure of thick sputtered Cu coatings. J. Vac. Sci. Technol., A. 1975;12:830-5.
[32] Rossiter P L. The electrical resistivity of metals and alloys. Cambridge: Cambridge University Press;1987.
[33] Zhang Q G, Zhan X, Cao B Y, Fujii M, Takahashi K, Ikuta T. Influence of grain boundary scattering on the electrical properties of platinum nanofilms. Appl. Phys. Lett. 2006;89:114102
[34] Veszelei M, Andersson K, Ribbing C-G, Järrendahl K, Arwin H. Optical constants and Drude analysis of sputtered zirconium nitride films. Appl. Opt. 1994;33:1993-2001.